

# COMPARISON OF SELECTIVE LASER MELTING OF 18Ni MARAGING STEEL BY PXL AND M2 CUSING

DANIEL KOUTNY, LIBOR PANTELEJEV,  
JAN TOMES, DAVID PALOUSEK

Brno University of Technology  
Faculty of Mechanical Engineering  
NETME Centre, Brno, Czech Republic

DOI: 10.17973/MMSJ.2016\_12\_2016191

e-mail: [daniel.koutny@vut.cz](mailto:daniel.koutny@vut.cz)

This study compares 18Ni maraging steel processing on two competitive SLM machines, PXL and M2 Cusing. For the production of samples, powder material from original machine supplier was used on each machine separately. Process parameters for the production of small thin-walled parts were set individually on each machine according to the recommendation of the device manufacturer. The basic mechanical properties of the produced materials were determined using tensile tests and hardness measurement. Metallographic and fractographic analyses were conducted by means of a light and scanning electron microscopes. In comparison to M2 Cusing, higher relative density achieving 99.9% in the volume of material, was measured on the thin walled samples of PXL. The reason is probably higher energy density during material processing. As a consequence, the specimens from PXL had slightly better mechanical properties.

## KEYWORDS

Selective Laser Melting, Maraging Steel, Microstructure, Mechanical Properties, Fractography

## 1 INTRODUCTION

SLM technology is no longer used in industry solely for rapid prototyping, but also finds use in manufacturing many more end parts. The main advantage is the possibility of production of parts more complicated in shape, which would be difficult or even impossible to achieve by conventional production methods, e.g. components with a complex internal structure, such as cooling channels or cellular lattice structures [Yadroitsev 2009].

Maraging steels are known for their excellent mechanical properties, which they reach thanks to the precipitation strengthening of martensitic microstructure during aging treatment [Yasa 2012]. This heat treatment is typical for maraging steels, even their name derives from "aging of martensite". [Jäggle 2014] found out that after the SLM process the material consists of a martensitic matrix with small regions of retained austenite. In later study, [Jäggle 2016] shown, that in this state, no precipitates in the material appear. Precipitates are formed during *age hardening*, specifically  $Ni_3Ti$ ,  $Ni_3Mo$  and  $Fe_7Mo_6$ . One of the first results of SLM processed 18Ni maraging steel were published by [Kruth 2005]. They produced samples reaching the ultimate tensile strength of 1410 MPa, Young's modulus of 162 GPa and the hardness 398 HV0.1. [Yasa 2009] measured similar hardness 376 HV0.5 and using precipitation hardening of 3h at 480°C increased the value to 572 HV0.5. On the other hand, a decrease of the impact energy (Charpy pendulum test) from 36.3 J to 10.1 J occurred. In further studies [Yasa 2010], [Yasa 2011] they conducted

more experiments with this material. Based on these tests, they selected precipitation hardening of 5h at 480°C as a suitable heat treatment for 18Ni maraging steel. After such modified heat treatment, ultimate tensile strength (UTS) of 1290 MPa was increased to 2216 MPa. The hardness increased from 40 HRC to 58 HRC, but there was a rapid decrease in elongation of the sample from 13% to 1.6%. Young's modulus also showed an increase from 163 GPa to 183 GPa. This is largely affected by heat treatment. An experiment similar to studies of Yasa was conducted by [Campanelli 2009] and [Casalino 2015]. They confirmed that the obtained relative density of the material increases with the supplied energy density. At a relative density higher than 99.7%, the produced material exhibited UTS 1085-1192, 30-35 HRC hardness and 5-8% elongation. Precipitation hardening of 6h at 490°C was used as heat treatment, which resulted to UTS 2097 MPa and hardness of 50 HRC as a maximum values of mechanical properties. Elongation after heat treatment was in the range of 4-6%. Unlike [Yasa 2010], [Kempen 2011], re-melting of each layer was not used in the production of samples for mechanical tests, which might have been the main reason for the different results. In studies of [Stanford 2008] and [Yasa 2010], inclusions were found in the microstructure, which gave impulse to further work of [Yasa 2011]. In this study they found out that the covering atmosphere during processing of 18Ni maraging steel has a significant role. Higher oxygen content in the  $N_2$  covering atmosphere increased thickness of oxidation layer on the surface layer of the components. The layer consists of  $Al_2O_3$  oxides and  $Ti_3O_5$  (prevailing oxide type in the layer), which even forms large inclusions of irregular shape in the part.

There are other studies in which 18Ni maraging steel using SLM processing has been described. [Campanelli 2010] and [Contuzzi 2013] focused on dimensional accuracy and cellular structures. [Delgado 2011] and [Hopmann 2015] compared the production of a part using SLM with the production using conventional methods.

Only one study focuses on a comparison of production on two different machines. [Yasa 2012] compared a part of the tests of the study [Yasa 2010] with newly conducted tests on a device from another manufacturer. It was equipped with a fiber laser, in contrast with previous studies in which the Nd:YAG laser was used. Interestingly, by means of the same hatching strategy, device with fiber laser achieved maximum relative density at lower energy density. As a possible reason the authors stated a lower beam diameter and a higher quality beam of the fiber laser. This study compares 18Ni maraging steel processing on two competitive SLM machines, M2 Cusing, manufacturer Concept Laser (CL), and PXL from Phenix Systems (PS). Different powder materials and manufacturing settings were used in particular cases. The production parameters were set for the manufacturing of small thin-walled parts in both cases. The study presents a comparison of the microstructures and mechanical properties of the samples.

## 2 MATERIAL AND METHODS

### 2.1 Metal powder

For the production of the samples, two types of powder material were used in this study. For the production on PXL the material labeled as ST2709B is used; material labeled as CL50WS is used for M2 Cusing. The quality of both is similar fulfilled the standard 1.2709, DIN X3NiCoMoTi18-9-5, 18Ni maraging (300), which is a high-strength, martensitic age hardenable steel. Chemical composition of evaluated materials denoted by suppliers is listed in Table 1.

**Table 1.** Chemical composition of powders

Weight %	CL 50WS (M2 Cusing)	ST2709B (PXL)
Fe	Balance	Balance
Ni	17.0 – 19.0	17.0 - 19.0
Co	8.5 - 10.0	9.0 - 11.0
Mo	4.5 - 5.2	4.0 - 6.0
Ti	0.8 - 1.2	0.9 - 1.1
Si	≤ 0.1	≤ 1
Mn	≤ 0.15	≤ 1
C	≤ 0.03	≤ 0.03
Cr	≤ 0.25	-
S	≤ 0.01	-
P	≤ 0.01	-

Powder from the two its producers was used for the analyses of particle size distribution, both in the virgin state (directly from the manufacturer) and after use and sieving the powder by standard means used in the manufacturing process. Analyses were performed using the analyzer Horiba LA-950.

**2.2 Fabrication of samples**

The samples were fabricated on two devices. The first one, Phenix Systems PXL is equipped with a fiber laser of maximum power 500 W and a wavelength of 1070 nm. The diameter of the laser beam is in the range of 70-80 micrometers. The second device is Concept Laser M2 Cusing, which uses a fiber laser with a wavelength of 1070 nm, but with a smaller maximum power of 400 W. The laser beam diameter is about 80 μm.

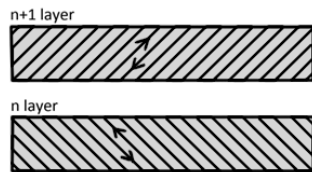


**Figure 1.** Laser scanning strategy

Both devices used for fabrication of samples layer thickness of 40 μm and inert nitrogen atmosphere. Oxygen level in M2 Cusing was kept below 1%; while in PXL the set point, to which the oxygen level is approaching, was 0.1%. During the production, heating of the base plate and chamber was not used. The general strategy used for laser processing of individual layers is shown on Fig. 1. This is the standard type of the hatching, wherein the adjacent laser vectors have opposite directions and the subsequent layer is rotated by 90°. This approach was used on both devices for fabrication of all samples, however, the values of hatching distance and other parameters differed. The different laser processing parameters and hatch distance used in particular devices are shown in Tab. 2.

**Table 2.** Different process parameters

Process parameters	M2 Cusing	PXL
Laser power [W]	180	220
Laser scanning speed [mm/s]	800	1200
Hatch distance [mm]	0.105	0.07

**2.3 Heat treatment**

The produced samples (thin wall sample further labeled as L3 and cylindrical billets used for mechanical testing) were annealed with 5-hour heating to a temperature of 830 °C and holding time of 30 min. Cooling was carried out in a closed

furnace, which was opened after reaching the 300°C, then the cooling process continued on air.

**2.4 Metallographic analysis**

The samples for microstructural analysis took shape of walls with the thickness of 2.5 mm. The plane observed during metallographic analysis was parallel to the build direction for all samples. The samples were analyzed by means of a light microscope in etched and non-etched state using metallographic microscope OLYMPUS GX 51. For a more detailed analysis of the microstructure, a scanning electron microscope ZEISS Ultra Plus was used.

Porosity in non-etched state was evaluated using the program ImageJ and the function *Analyze Particles*. The resulting porosity was determined as an average value asquired from three measured areas. The selected areas had the form of rectangles over the entire wall thickness, and they were of the same size and position on all metallographic samples.

**2.5 Mechanical properties**

The SLM samples for tensile testing were built in the form of cylindrical billets with a diameter of 20 mm and length of 95 mm. After the production, they were heat treated and machined to form a standard sample for tensile test, with specimen having a nominal diameter of 8 mm and the gauge length of 40 mm (according to DIN 50125). Tensile tests were performed on the machine Zwick Z250 at room temperature with testing speed of 1 mm/min. Measurement of hardness HV 0.3 was performed using test LECO LM 274 AT hardness tester.

**3 RESULTS AND DISCUSSION**

**3.1 Powder analysis**

The basic statistical values of the analyzed particle sizes of both used powders are shown in Tab.3 and Fig. 2.

**Table 3.** Statistical parameters of particle size of powder material

Particle size [μm]	CL50WS (M2 Cusing)		ST2709B (PXL)	
	new	sieved	new	sieved
Median	29.498	27.430	10.438	7.383
Standard dev.	8.657	7.689	3.595	0.712
Modus	28.075	27.602	10.782	7.317
d <sub>10</sub>	19.470	18.422	6.150	6.394
d <sub>50</sub>	28.402	26.453	10.031	7.326
d <sub>90</sub>	41.047	37.751	15.193	8.476

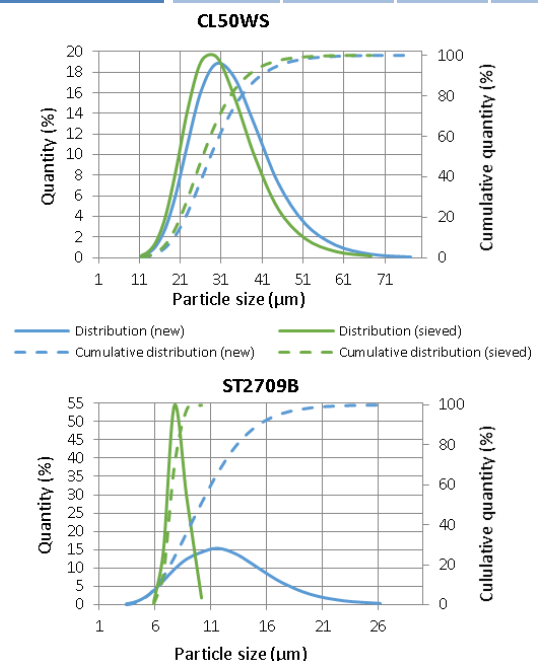


**Figure 2.** Particle size distributions of CL50WS (Concept Laser) and ST2709B (Phenix Systems) powders

It is obvious based on obtained data that the characteristic of the two powders varies significantly. Powder ST2709B (Phenix Systems) exhibited significantly smaller particles, than CL50WS powder. In addition, the new powder ST2709B has much wider particle size distribution in comparison with the sieved one. Apparently, a sieve with very small mesh size (app. 10 μm) was chosen to be employed there. Small particle size dispersion generally leads to higher porosity of parts. However, this should not represent a problem in such small particle sizes.

The powder CL50WS (Laser Concept) has a broader particle size distribution with an average size considerably higher than the powder produced by PS. The difference of particles size is also clearly visible in Fig. 3. It is obvious that powders are primarily intended for the production of different layer thickness. In the process, the ST2709B powder can be used from the layer thickness of 15 micrometers. The CL50WS powder is suitable for producing a layer thickness of 40 micrometers. It is obvious that sieving of the powder CL50WS has not such a significant impact on particle size distribution contrary to the case of ST2709B powder (Fig. 2). Nevertheless, the characteristic of CL50WS powder is slightly modified by sieving.

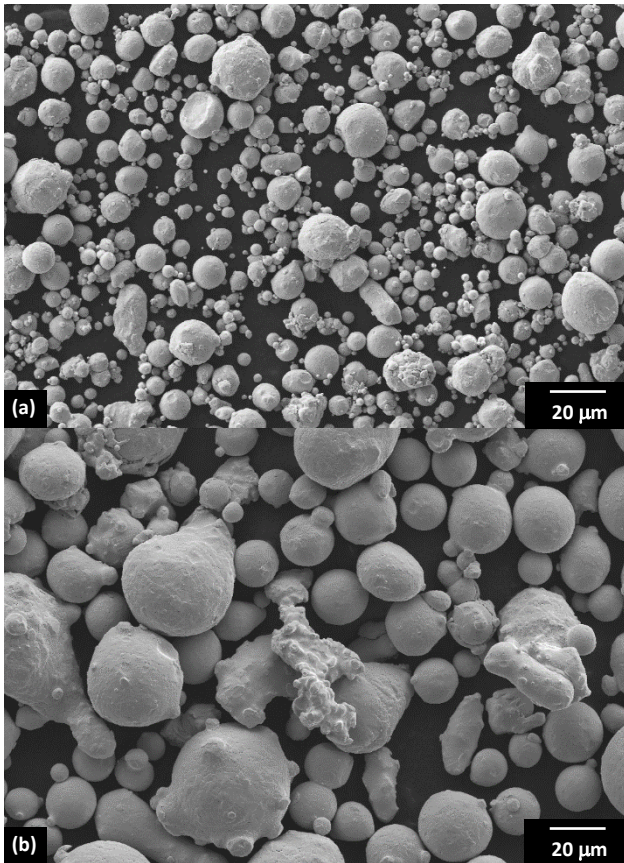


**Figure 3.** SEM images of powder materials (a) ST2709B, (b) CL50WS

### 3.2 Metallographic analysis

The first sample, in this study labeled as L1, was made on the device PXL. Two additional ones (L2, L3) were produced on the M2 Cusing. Samples L1 and L2 are in a condition without additional heat treatment, the sample L3 was annealed directly after SLM production. Fig. 4 shows microstructure of samples L1 and L2 in non-etched state.

**Table 4.** Porosity of metallographic specimens

	L1	L2	L1w
--	----	----	-----

Porosity [%]	0.17	0.85	0.06
σ [%]	0.07	0.22	0.02

The microstructure in non-etched state exhibited a significant difference in the amount of porosity and its distribution at individual samples. The sample L1 shows minimal amount of pores in inner volume, but higher porosity with pore size of about 0.1 mm was found close to the surface (Fig. 4a). The porosity of the sample L2 is not located to the surface layer only and it is present in whole volume of the material (Fig. 4b). The results of porosity measurement for all tested thin wall samples are listed in Table 4. The porosity of the sample L1 excluding the subsurface pores (labeled as L1w) is given in the table as well for comparison. This value does not take into account the influence of sample dimension and it was assumed as porosity of the cylindrical samples used for the tensile test at which the surface layer was machined.

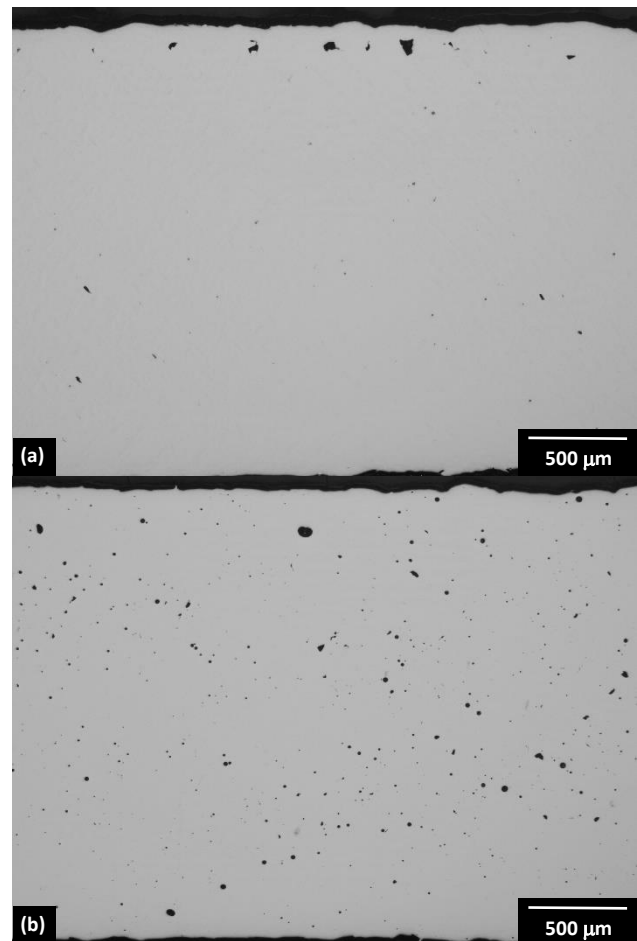


**Figure 4.** Pictures of metallographic samples; (a) L1; (b) L2.

Porosity in SLM processed materials is affected by process parameters, as a laser power, laser scanning speed and hatch distance. As an indicator, the laser energy density  $E$  given by formula (1) may be used. Parameters used in M2 Cusing device gives the resulting energy density of 53.6 J/mm<sup>3</sup>, while the samples made in PXL had higher energy density of 65.5 J/mm<sup>3</sup>. As seen from Fig. 3, the laser energy density has a direct impact on the porosity.

$$E = \frac{Lp}{Ls \cdot Hd \cdot Lt} \text{ [J/mm}^3\text{]} \quad (1)$$

$Lp$  – laser power;  $Ls$  – laser scanning speed;  $Hd$  – hatch distance;  $Lt$  – layer thickness

On Fig. 5 the microstructure of individual samples in etched state is shown. It is apparent that the metal powder has been



completely melted through and formed the linear regions corresponding to the trajectory of the laser movement during hatching. It is obvious that the individual sintered vectors successively overlap according to the used hatching

strategies (Fig. 1). Due to very fine microstructure of produced samples and inherent limitations of light microscopy the scanning electron microscopy was used for detailed microstructural analysis (Fig.6-8).

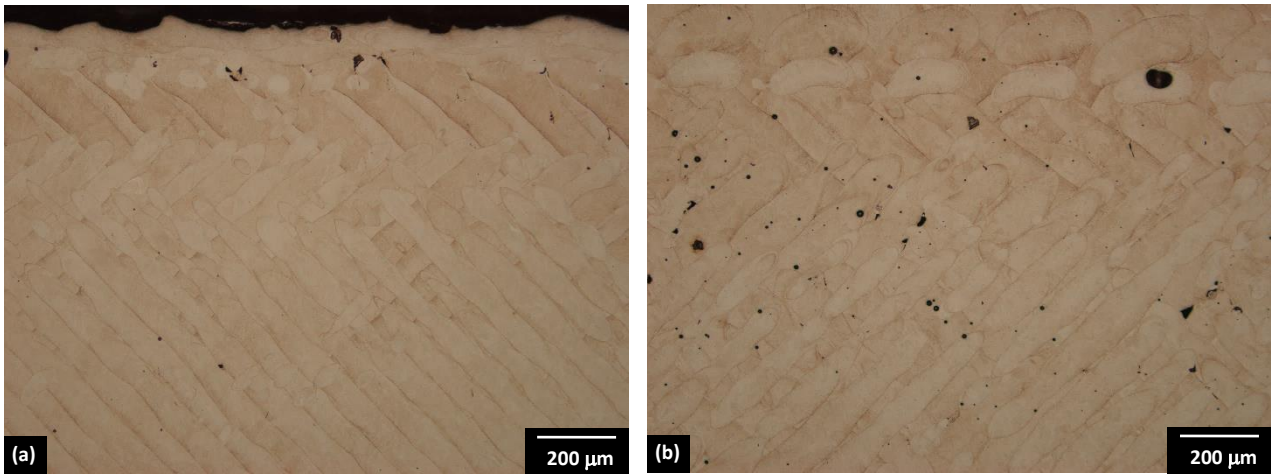


Figure 5. Microstructure of samples L1 a), L2 b) and L3 c) after etching

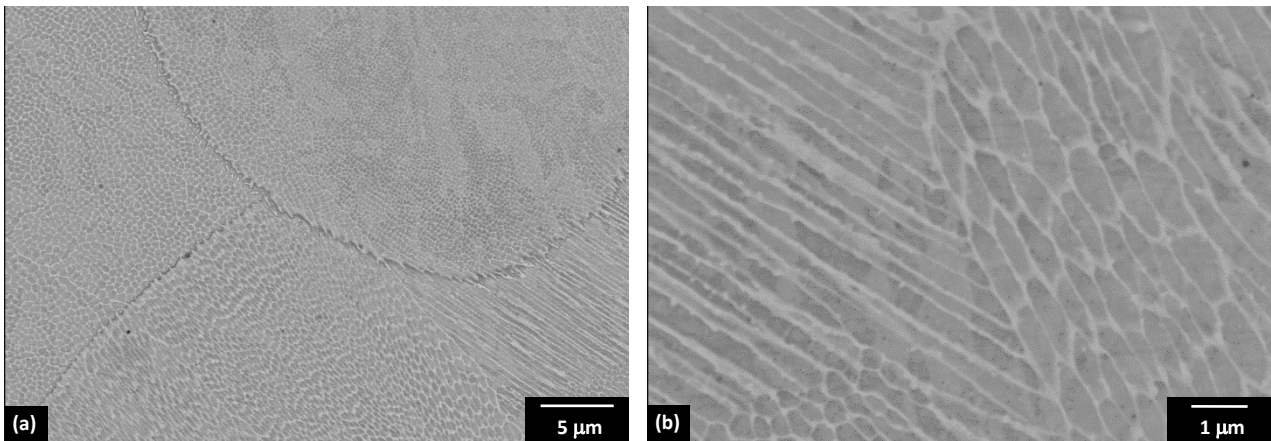


Figure 6. SEM picture of specimen L1 with various magnification of microstructure, a) overview, b) details of boundary

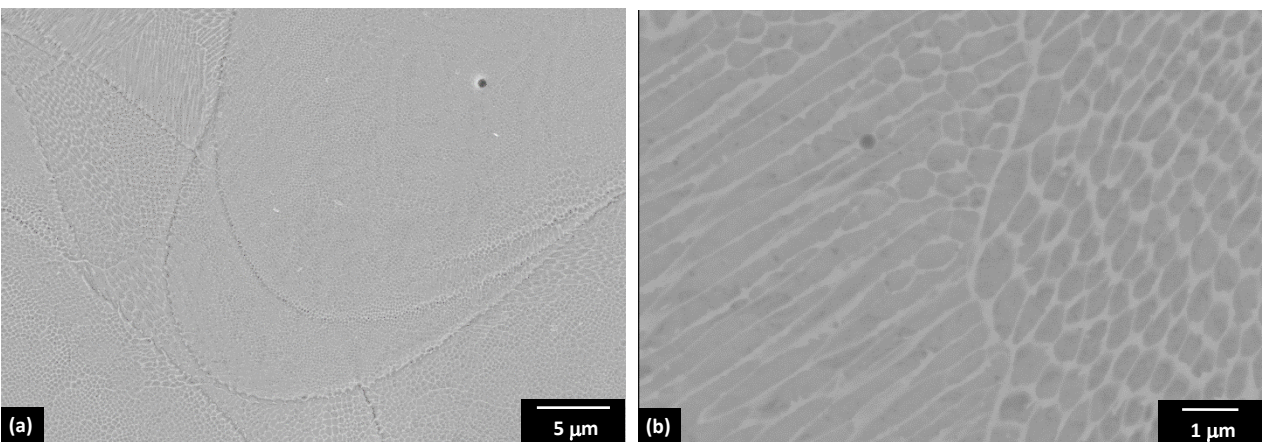


Figure 7. SEM picture of specimen L2 with various magnification of microstructure, a) overview, b) details of boundary



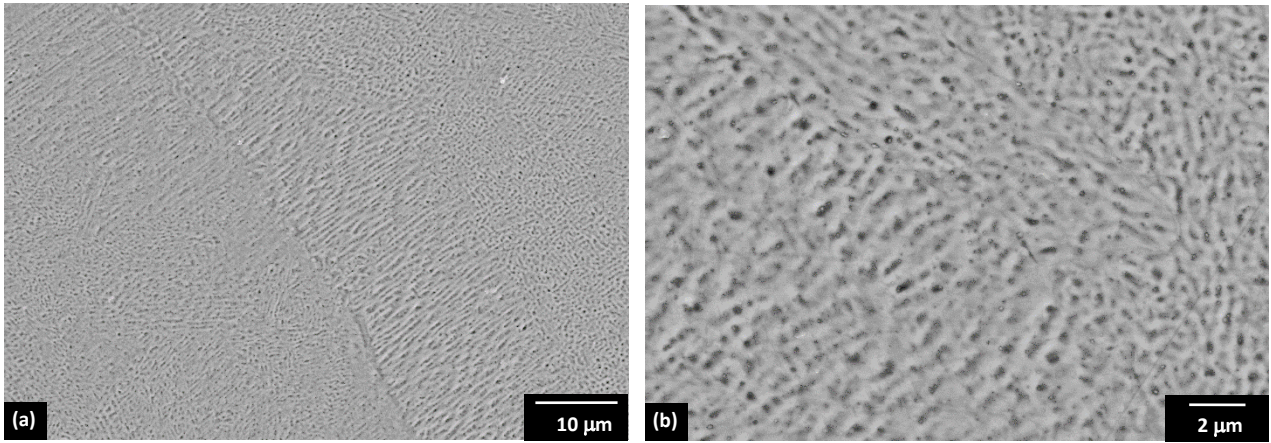


Figure 8. SEM picture of specimen L3 with various magnification of microstructure, a) overview, b) details of boundary

It is obvious that the structure is very fine consisting of cells with thin boundaries. Tendency to elongation of the cells is locally visible as well (Fig. 6b and 7b). Due to very high cooling/solidification rate during the SLM process, formation of a lath martensite is suppressed. Figure 8 clearly shows that the heat treatment after SLM process significantly influences the microstructure of the material. The growth of cell boundaries thickness at the expense of its inner volume is clearly visible (compare Figs. 7 and 8).

### 3.3 Tensile testing

Results of tensile test of individual samples are listed in Tab.5 as an average value determined from three measurements. It is obvious that the selected annealing used in this study has rather a negative effect on the strength and hardness, if compared with literature data [Kempen 2011], where UTS over 2000 MPa was achieved for heat treated samples.

Table 5. Comparison of mechanical properties

Machine	Modulus of elasticity E (GPa)	0.2% Proof stress Rp0,2 (MPa)	Ultimate tensile strength (MPa)	Elongation A (%)	Area reduction Z (%)	Hardness HV 0,3(HRC)
PXL	180	821	1175	9.3	30.7	353 (36.0)
M2	152	800	1116	6.9	28.8	335 (33.3)

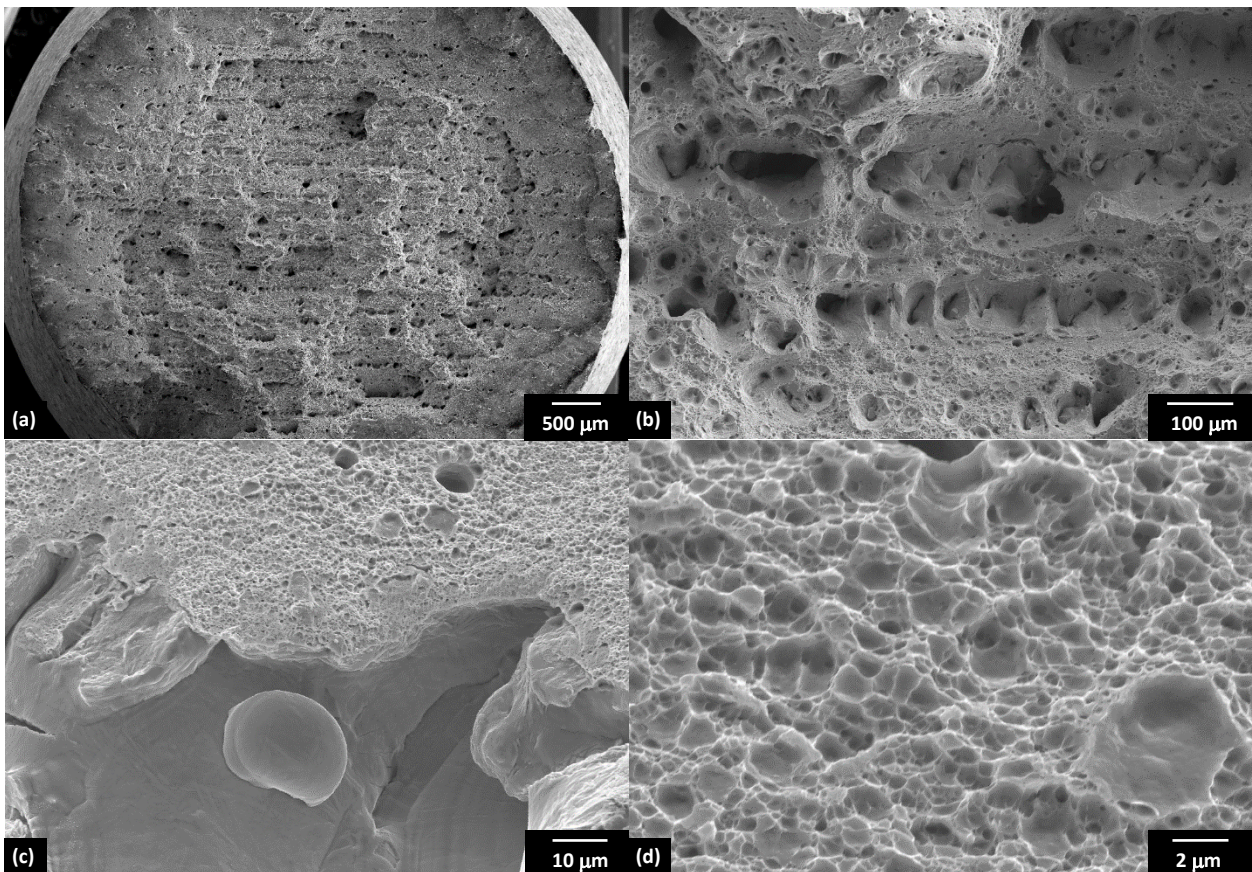
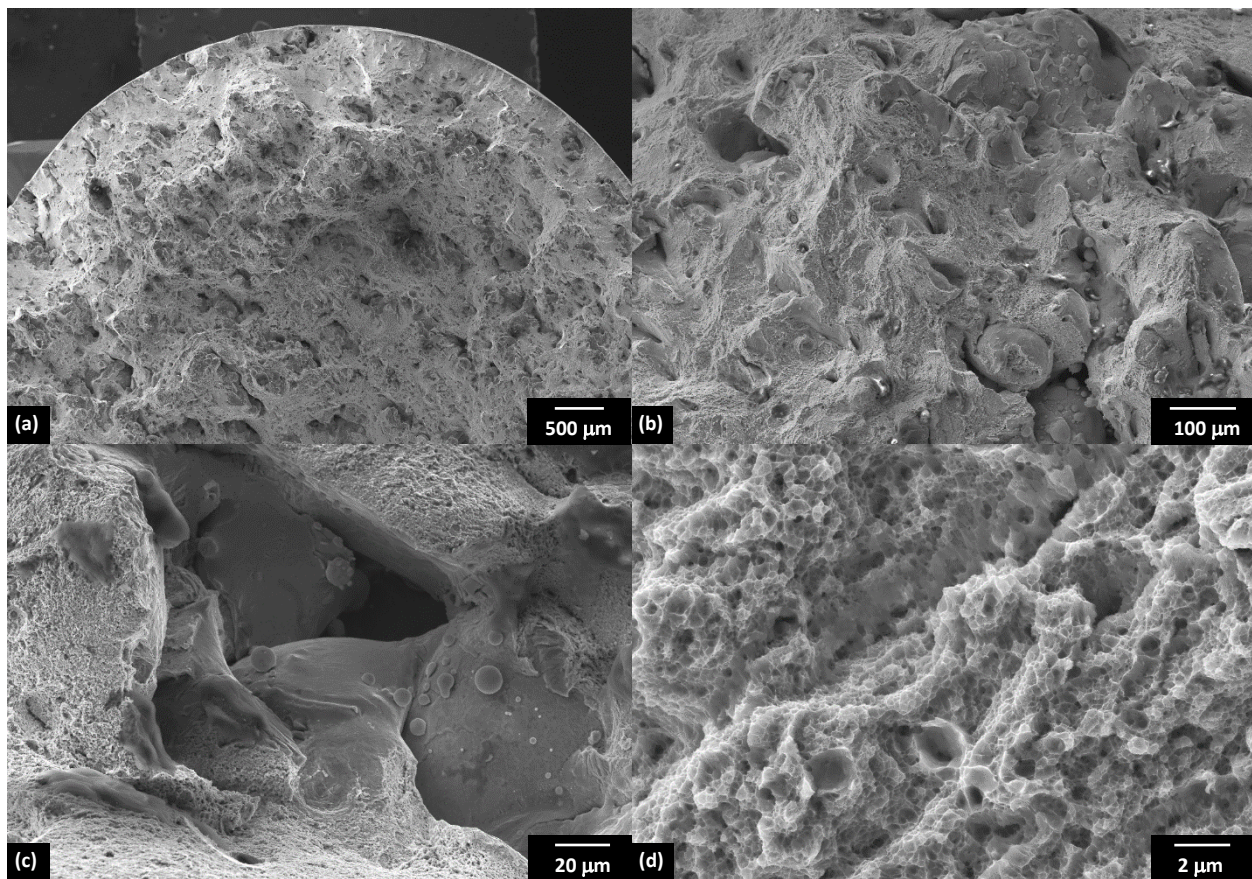


Figure 9. SEM pictures of fracture surface of specimens M2





**Figure 10.** SEM pictures of fracture surface of specimens PXL

Mechanical properties are strongly influenced by porosity, therefore higher porosity in M2 Cusing could be the reason for slightly lower UTS values of M2 samples. Slight difference in UTS values corresponds to lower values of hardness (Table 5). Fractographic analysis was performed on broken samples after tensile testing using scanning electron microscope. Relatively uniform distribution of micro defect was found on the fracture surface of samples M2 (Fig. 9). The arrangement of defects corresponds to scanning strategy because the defects are formed in parallel lines which are perpendicular to build direction.

Unmelted particles were found on the fracture surface inside shrinkages (Fig. 9b, c). Fracture surface of the M2 samples is of ductile character with dimple morphology, whereas present dimples are tiny and shallow (Fig. 9d). Similar fracture behavior was found in the case of PXL samples. Arrangement of micro defects is little bit different if compared with samples M2. The uniformity of micro defects/shrinkages was not observed in the case of PXL samples (Fig. 10 a, b). Detailed assessment of the fracture surfaces revealed unmelting metal powder particles inside shrinkage (Fig. 10c) and tiny and shallow ductile dimples (Fig. 10d) as in the case of M2 samples.

It is obvious that the defects originated during SLM process, most probably due too wide hatching distance causing insufficient melting of the adjacent scanning tracks. When assessing the fracture surfaces of all broken tensile samples, it can be said that the nature of the failure is very similar; in local areas the fractures are ductile, however, interrupted by a number of micro-defects distributed over the cross-section of the sample.

Based both on fractographic and metallographic analyses, it is obvious that the scanning strategies and other process parameters optimized for the production of thin-walled parts are not entirely suitable for the production of bulk structural

part (cylindrical billets in this case), because it leads to formation of significant porosity.

#### 4 CONCLUSION

With respect to the fact that different process parameters and metal powders with very different particle size distribution used for sample production on different SLM machines (Phenix Systems PXL and Concept Laser M2 Cusing), the values of UTS and hardness vary on the level about 10 %. Presence of metallurgical defects was found on the fracture surface independent on used SLM device or processing parameters. Mechanical properties achieved for the materials in annealed states are the same or lower if compared with the values of thermally unprocessed material reported in the literature.

Samples produced on PXL with smaller hatching distances or rather higher laser energy density reached lower porosity. The value of the relative density (surface porosity is excluded, due to machining process of billets for tensile testing) was over 99.9% which resulted in slightly better mechanical results compared to M2 Cusing. The low porosity in case of PXL samples could also have been affected by lower mean particle size of the powder material.

#### ACKNOWLEDGEMENTS

The research leading to these results has received funding from the Ministry of Education, Youth and Sports under the National Sustainability Programme I (Project LO1202) and Czech Science Foundation project GA15-23274S and faculty research project project FSI-S-14-2332.

## REFERENCES

- [Campanelli 2009] Campanelli, S.L., et al. Manufacturing of 18 Ni Marage 300 Steel Samples by Selective Laser Melting. In: Advanced Materials Research. 2009, vol. 83-86, p. 850-857. DOI: 10.4028/www.scientific.net/amr.83-86.850.
- [Campanelli 2010] Campanelli, Sabina Luisa, et al. Capabilities and performances of the selective laser melting process. INTECH Open Access Publisher, 2010.s
- [Casalino 2015] Casalino, G., et al. Experimental investigation and statistical optimisation of the selective laser melting process of a maraging steel. Optics & Laser Technology, 2015, 65: 151-158.
- [Contuzzi 2013] Contuzzi, Nicola, et al. Manufacturing and Characterization of 18Ni Marage 300 Lattice Components by Selective Laser Melting. Materials, 2013, 6.8: 3451-3468.
- [Delgado 2011] Delgado J., et al. Comparison of forming manufacturing processes and selective laser melting technology based on the mechanical properties of products. In: Virtual and Physical Prototyping. 2011. 6:3, 167-178, DOI: 10.1080/17452759.2011.613597
- [Hopmann 2015] Hopmann C, et al. Surface quality of profile extrusion dies manufactured by Selective Laser Melting. In: RTeJournal - Forum für Rapid Technologie. 2015. (urn:nbn:de:0009-2-42900)
- [Jäggle 2014] Jäggle, E. A., et al. Precipitation and austenite reversion behavior of a maraging steel produced by selective laser melting. In: Journal of Materials Research. 2014. 29(17), 2072-2079. doi:10.1557/jmr.2014.204.
- [Jäggle 2016] Jäggle, E. A., et al. Precipitation Reactions in Age-Hardenable Alloys During Laser Additive Manufacturing. 2016, 68(3), 943-949. DOI: 10.1007/s11837-015-1764-2. ISSN 1047-4838.
- [Kempen 2011] Kempen, K., et al. Microstructure and mechanical properties of Selective Laser Melted 18Ni-300 steel. In: Physics Procedia. 2011, vol. 12, p. 255-263. DOI: 10.1016/j.phpro.2011.03.033.
- [Kruth 2005] Kruth, Jean-Pierre, et al. Benchmarking of different SLS/SLM processes as rapid manufacturing techniques. 2005.
- [Stanford 2008] Stanford, M. K., et al. An investigation into fully melting a maraging steel using direct metal laser sintering (DMLS). In: Steel research int. Special Editions Metal forming Conference 2008. 2008. 79(2):847-852.
- [Yadroitsev 2009] Yadroitsev, Igor. Selective laser melting: direct manufacturing of 3D-objects by selective laser melting of metal powders. Saarbrücken: LAP Lambert, c2009, iv, 266 s. ISBN 978-3-8383-1794-6.
- [Yasa 2009] Yasa, Evren, et al. Experimental investigation of Charpy impact tests on metallic SLM parts. In: Innovative Developments in Design and Manufacturing Advanced Research in Virtual and Rapid Prototyping. 2009. p. 207-214.
- [Yasa 2010] Yasa, Evren, et al. Microstructure and mechanical properties of Maraging Steel 300 after selective laser melting. In: Proceedings of the 21st Annual International Solid Freeform Fabrication (SFF) Symposium, University of Texas, Austin. 2010. p. 383
- [Yasa 2011] Yasa, Evren, et al. Investigation on the inclusions in maraging steel produced by Selective Laser Melting. In: Innovative Developments in Virtual and Physical Prototyping: Proceedings of the 5th International Conference on Advanced Research in Virtual and Rapid Prototyping, Leiria, Portugal, 28 September-1 October, 2011. CRC Press. 2011. p. 297.
- [Yasa 2012] Yasa, Evren, et al. Selective Laser Sintering/Melting and Selective Laser Erosion with Nd: YAG Lasers. Journal of Optics Research, 2012, 14.3/4: 211.

## CONTACT:

Ing. Daniel Koutny, Ph.D.  
Brno University of Technology  
Faculty of Mechanical Engineering  
Institute of Machine and Industrial Design  
Technická 2896/2, 616 69 Brno, Czech Republic  
e-mail : [koutny@fme.vutbr.cz](mailto:koutny@fme.vutbr.cz)  
Tel. : +420541143356  
<http://www.uk.fme.vutbr.cz/>